

Quantum Down Conversion and Multipartite Entanglement via a Mesoscopic SQUID Ring

P.B. Stiehl, M.J. Everitt, T.D. Clark, and C.J. Harland
Centre for Physical Electronics and Quantum Technology,
School of Engineering, University of Sussex, Brighton, Sussex BN1 9QT, U.K.

J.F. Ralph
Liverpool University, Brownlow Hill, Liverpool, L69 3GJ, U.K.
(Dated: 22 nov 2004)

In this paper we study, by analogy with quantum optics, the SQUID ring mediated quantum mechanical interaction of an input electromagnetic field oscillator mode with two or more output oscillator modes at sub-integers of the input frequency. We show that through the non-linearity of the SQUID ring multiphoton down conversion can take place between the input and output modes with the resultant output photons being created in an entangled state. We also demonstrate that the degree of this entanglement can be adjusted by means of a static magnetic flux which controls the strength of the interaction between these modes via the SQUID ring.

I. INTRODUCTION

Over the last few years there has been a rapidly growing interest in quantum technologies, particularly for the fields of quantum information processing and quantum computing^{1,2}. This has been aided both by the creation of key algorithms^{3,4} and by improvements in experimental technique. A range of approaches, involving different physical disciplines, have been adopted in the pursuit of these technologies but at the basis of each is the concept of using entangled states of quantum objects^{1,2}. The creation of entangled states, and the exploitation of their properties, are therefore seen as fundamental to successful progress in these technologies. In particular, it is clear that there exists a need to develop systems or devices through which the degree of entanglement between quantum objects can be actively controlled. In this paper we show how the intrinsic non-perturbative behaviour of a quantum SQUID ring (here, a thick superconducting ring enclosing a Josephson weak link device) can be used to achieve this goal, taking as our specific example entanglement between photon states.

Interest in the use of SQUID rings (and other weak link circuits) as quantum logic devices has been stimulated by recent experiments to probe superposition of states in these systems^{5,6,7,8,9,10}. Furthermore, other recent experiments have been performed that show coherent dynamics of superconducting flux qubits coupled to individual harmonic oscillators¹¹. Building on this background, and previous theoretical work by us on the coupling of SQUID rings to electromagnetic (em) fields¹², we consider the process of photon down conversion via a mesoscopic SQUID ring. Specifically, by analogy with the field of quantum optics, we demonstrate that the ring may be viewed as a non-linear medium which can down convert photons from one frequency (input field oscillator mode) to another lower frequency and generate entangled photons (output field oscillator modes), as is often performed in quantum optics experiments¹³. An analysis

of multiple output modes is important since it allows us to understand the way in which several quantum circuits may be entangled – an important issue in quantum technologies – for example, as entanglement registers in quantum computing. We also note that by coupling in a larger number of field modes we change the position (in x) of the splittings in the spectrum of the Hamiltonian for the composite system. We consider, therefore, that it is by no means trivial to assume that we can simply extend the results of our previous work^{12,14}. As we have shown by computation, in a three mode system (two em field modes plus one SQUID mode) entanglement can be adjusted through the control of a static bias flux Φ applied to the ring. From an experimental viewpoint, in this system down conversion processes are relatively easy to observe¹⁵ at least for the situation where microwaves (input electromagnetic field in the range of a few to 10 GHz) are down converted to radio frequencies (rf output mode 1 to 20 MHz)¹⁵. We note that microwave photons are difficult to transport, which could be problematic for some applications in quantum communication. By implication, but not calculated in this work, it should also prove possible to observe up conversion processes involving significant frequency ratios between input and output. However, the ultra low noise electronics required for the output stage in an experiment of this type (say, for inputs at rf and outputs at microwave frequencies) is much more difficult to engineer than at the much lower radio frequencies. Having observed down conversion in the experiments at Sussex¹⁵, we tried to emulate this behaviour theoretically. However, such large frequency differences (a few GHz input, a THz SQUID ring characteristic oscillator frequency and a few MHz output) was found to be computationally intractable at this time. Bearing this in mind, and considering the interest currently shown in quantum computing, we chose to demonstrate in this paper that SQUID rings can act as devices which mediate large ratio frequency down conversion that is also computationally tractable. Moreover,

form multiple output modes we demonstrate that the down converted photons are entangled together. In our computations we have modelled the ω eld oscillator modes as equivalent resonant LC circuits. Experimentally, this could be realised by utilising real LC circuits constructed from superconducting material to minimise decoherence. Alternatively we could use a transmission line comprising a series of coupled superconducting LC resonators^{15,16}.

From an experimental perspective, it is interesting to note that there has already been some progress made in realising simple quantum circuits systems relevant to the work presented in this paper. In this regard there are now several examples of coupled superconducting qubits (here the SQUID ring is, to all intents and purposes, a flux qubit). These include fixed coupling flux qubits¹⁷, current biased Josephson-junction qubits that are either coupled capacitively¹⁸ or via a connecting superconducting loop¹⁹. Recently, there has even been an example of tripartite quantum entanglement in macroscopic superconducting circuits²⁰. Moreover, an application that relates very strongly to the circuit systems presented in this work utilised a SQUID ring to mimic a simple harmonic oscillator. This device was then coupled, quantum coherently, to a superconducting flux qubit¹¹. However, although the physics of all these systems is similar, in this work we have chosen to consider a superconducting circuit coupled to quantum electrodynamic degrees of freedom, i.e. photons in a cavity. Recently it has been shown that a superconducting qubit can be quantum coherently coupled to an on-chip cavity¹⁶. Furthermore, we note that superconducting devices, which can be coupled to these and more exotic systems, such as GHz nanomechanical resonators²¹, are not only easy to fabricate, but are adaptable to a wide variety of applications.

In this work we first investigate, from a full quantum mechanical viewpoint, the simplest down conversion and entanglement process, involving one input photon at a given frequency and two output photons at half this input frequency. To the limits of the computational power available to us, we extend our theoretical investigation of such down conversion processes to that of generating four output photons, each at a quarter of the frequency of the input photon (i.e. a four photon down conversion). Within the Adami-Cerf criterion^{22,23,24} we show that entanglement exists between any one of these output oscillator modes and the rest of the system (i.e. SQUID ring and input oscillator mode). This implies that all the output modes will be entangled with each other, as well as to the rest of the coupled system. While this multipartite entanglement may not be as strong as some bipartite entanglements, such as Bell States, it is a key component in certain requirements in quantum computation, such as entanglement registers, where a large number of qubits are entangled together to generate a total entangled state for the process of computation. It is this idea that is responsible for the (as yet in principle) power of quantum computing over modern day, classical computers. Also, the question of characterising entanglement in multipartite

quantum systems is still very much an open one. Whilst each measure agrees as to whether the state vector of a given system is separable, or maximally entangled, they do not, in general, provide an ordering that can be used to quantify entanglement of more general states. In this paper we have chosen to use an entanglement measure that gives us an idea of the distribution of the quantum correlations that exist in our example multipartite systems. However, as we have not produced maximally entangled states it is not possible to quantify absolutely the level of entanglement present. We note that for a simpler system, controlled via a dynamic flux bias²⁵, we have shown that it is possible to create a maximally entangled state between a SQUID ring and an ω eld mode. It may be that similar methods could be used in these composite systems to produce such states of maximal entanglement. Unfortunately computations with time dependent Hamiltonians are far harder to solve than the static cases presented in this paper, and are beyond the limit of current computational power.

For the example of the two photon process we consider the effect of dissipation on the coherent evolution of the coupled (entangled) system. By extension, we show by computation that much higher order (i.e. more than our computed four photon case) down conversions may prove possible experimentally. To this effect we provide a further example of down conversion by a factor of twenty between the input ω scillator mode and an output ω mode. However, both due to limitations in computer power, and a still insufficient understanding of entanglement in many particle (multipartite) quantum systems, we have not proceeded any further in characterising this high order example.

II. THEORETICAL MODEL

In our theoretical treatment of the interaction of quantised ω scillator modes (photons) with a mesoscopic quantum mechanical SQUID ring we model the ω eld modes as parallel LC resonators, as a simple and convenient way of parameterizing the (physical) cavity modes coupled to the SQUID ring. The scheme we have adopted is shown diagrammatically in figure 1 for the simpler, two photon, down conversion process. In this example the input photon frequency is $\omega_{e1} = 2$ while the two (identical) output frequencies are $\omega_{e2} = 2$ and $\omega_{e3} = 2$ such that $\omega_{e2} = \omega_{e3} = 0.5\omega_{e1}$. Here, the SQUID ring characteristic oscillator frequency is $\omega_s = 2 = 1/2 \omega_{sC_s}$ for a ring inductance and a weak link capacitance of L_s and C_s , respectively. In our calculations we treat this system fully quantum mechanically by assuming an operating temperature T such that $\hbar\omega_s \gg k_B T$; $\hbar\omega_{e1} \gg k_B T$ and $\hbar\omega_{e2,3} \gg k_B T$ are all much greater than $k_B T$ for ω eld mode inductances and capacitances L_{e1} and C_{e1} (where, generally, $i = 1; 2; 3; \dots$). In this model system the coupling between the SQUID ring and the oscillator

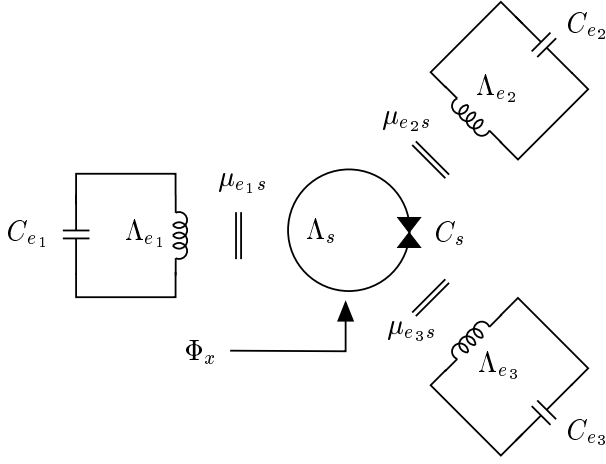


FIG. 1: Schematic of a four mode system comprising three electromagnetic field modes inductively coupled to a mesoscopic SQUID ring.

modes is taken to be inductive. As can be seen in figure 1, we have chosen to couple these circuits so that all interactions between the field modes are performed via the SQUID ring. In this four mode system (i.e. three field modes plus one SQUID mode) the static flux Φ_x applied to the ring can be used to control the level of interaction between the input field mode and an output field mode of the system. In a specific example in this paper, as an extension of previous work¹², we demonstrate that the behaviour of coupled SQUID ring-field mode systems is, in general, very strongly dependent on this control ux. Although this aspect of our investigations is an extension of the results of our previous papers^{12,14}, it is important to show that this dependence remains valid for the kind of multi-component circuits that would appear to be required in the quantum technologies currently being pursued^{1,2,5,6,7,8,9,10,11,24}.

The Hamiltonian for the coupled system of figure 1 is made up of the uncoupled Hamiltonians for each mode together with a set of interaction terms. For each field mode (both input and output) the Hamiltonian takes the form¹²

$$H_{e_i} = \frac{Q_{e_i}^2}{2C_{e_i}} + \frac{\phi_{e_i}^2}{2\Lambda_{e_i}} \quad (1)$$

where, again, $i = 1, 2, 3, \dots$, while for the SQUID ring we use the standard, time independent, lumped component circuit Hamiltonian^{26,27} (the wavelengths of the photon modes being very much larger than the dimensions of the mesoscopic SQUID ring circuit). Specifically

$$H_s = \frac{Q_s^2}{2C_s} + \frac{(\phi_s - \Phi_x)^2}{2\Lambda_s} \sim \cos 2\pi \frac{\phi_s}{\phi_0} \quad (2)$$

In this description ϕ_s (the magnetic flux threading the SQUID ring) and Q_s (the electric displacement flux between the electrodes of the weak link) are the conjugate variables for the ring, $\phi_0 = \Phi_0/2$ is the matrix element

for Josephson pair tunnelling through the weak link (of critical current $I_c = 2e\phi_0$) and $\phi_0 = \hbar/2e$ is the superconducting flux quantum. From the perspective of the work presented in this paper, the Josephson cosine term in the SQUID ring Hamiltonian (2) allows for non-perturbative behaviour to all orders in the coupled system of figure 1. In turn, this means that in interactions between a quantum SQUID ring and external fields, non-perturbative, multiphoton absorption/emission processes tend to dominate within an exchange region¹².

To illustrate the form of the solutions to the time independent Schrödinger equation for a SQUID ring, using the Hamiltonian (2), we show in figure 2 (a) the first four eigenenergies ($s = 0, 1, 2, 3$) as a function of external flux Φ_x for a typical mesoscopic quantum SQUID ring with parameters¹² $C_s = 5 \times 10^{-15}$ F, $\Lambda_s = 3 \times 10^{-10}$ H (giving a characteristic SQUID ring oscillator frequency of 130 GHz, this is much smaller than the superconducting energy gap in, for example, Niobium, that is often used to fabricate SQUID circuits) and $\phi_0 = 0.035 \phi_0^{\text{Nb}} \approx 0.035 \times 2.07 \times 10^{-10}$ Wb, equivalent to a Josephson frequency of 700 GHz, which is not unrealistic when compared to those used by Friedman et al⁶ (2 THz) and Orlando et al²⁸ (2.12 THz). These frequencies should be sufficient to avoid thermal excitations for any experiments performed at 40 mK, a temperature easily obtainable in modern dilution refrigerators. If we assume that the Josephson weak link in the SQUID ring is of the tunnel junction type with, typically, an oxide tunnel barrier of dielectric constant 10, then the junction dimensions will be close to 0.2 μm square, which can be fabricated using current lithographic and thin film techniques. Furthermore, with $\phi_0 = 0.035 \phi_0^{\text{Nb}}$, and these dimensions, the corresponding Josephson critical current density is $4 \text{ kA}/\mu\text{m}^2$ which appears suitable for SQUID rings operating in the quantum regime. In addition to the ring eigenenergies, we also show in figure 2 (a) the harmonic oscillator field mode eigenenergies of e_1 ($\sim \phi_{e_1}^2$, $s = 0, 1, 2, \dots$) (dotted) and $e_{2,3}$ ($\sim \phi_{e_{2,3}}^2$, $s = 0, 1, 2, 3, \dots$) (dashed). In figure 2 (b) we show the eigenenergies of the total coupled system. We note that at the level of capacitance chosen for the SQUID ring the energy splittings where the field mode energies and the ring energies cross are very small. In figure 2 (b) almost all these splittings are unresolved on this scale but at sufficient resolution all would be discernible.

Provided that we disallow any direct interaction between the field mode oscillators (this being our assumption) and a situation which is easy to establish experimentally), the coupling terms are given by

$$H_{e_i s} = \frac{e_i \phi_s}{\Lambda_{e_i}} (\phi_s - \Phi_x) \phi_{e_i};$$

where the $e_i \phi_s$ are the fractions of magnetic flux coupled inductively between any one of the field mode oscillators and the SQUID ring. The total system Hamiltonian H_t

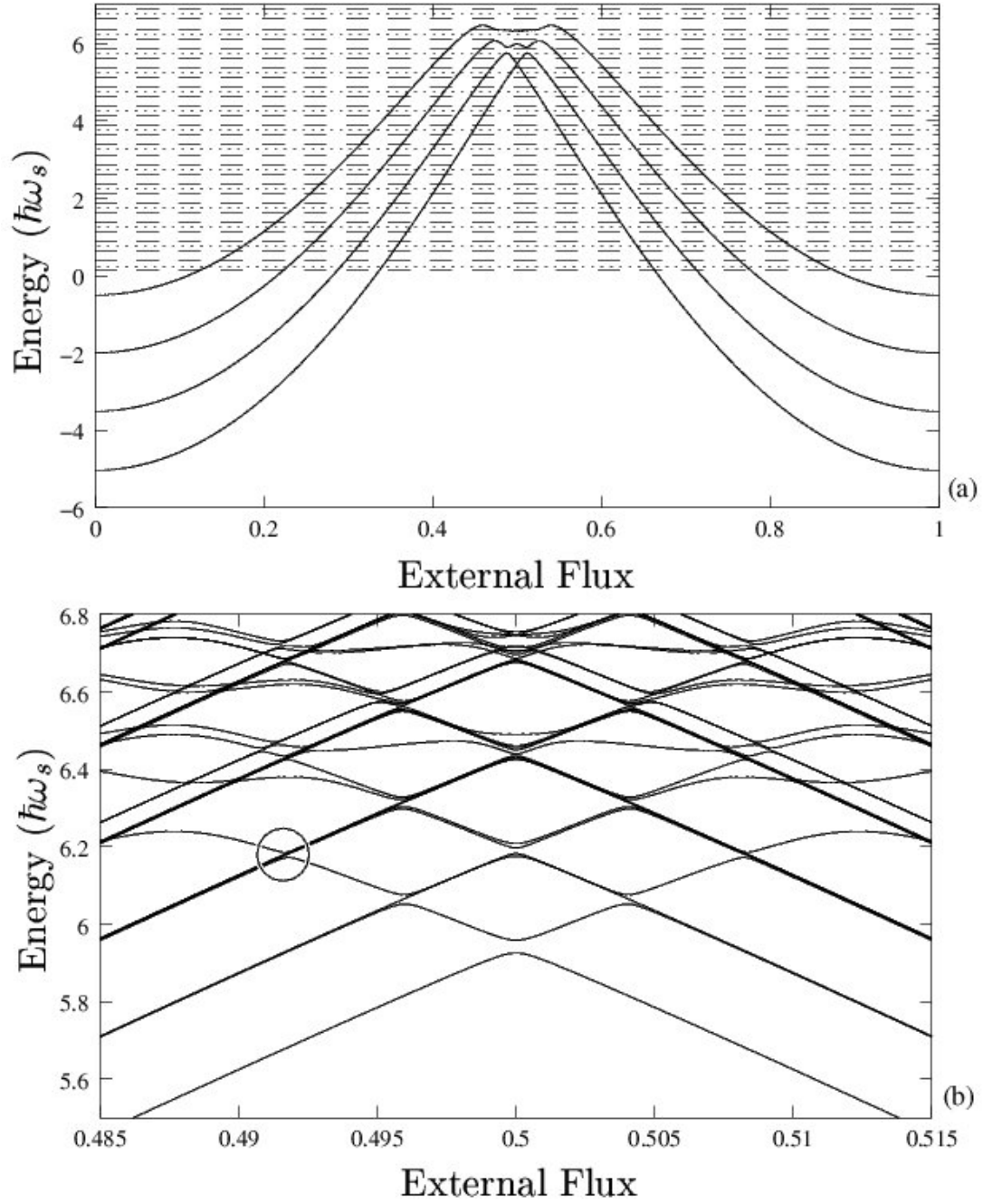


FIG. 2: (a) the eigenenergy spectrum of an uncoupled mesoscopic SQUID ring at $T = 0K$ as a function of external bias flux (solid lines) together with the harmonic oscillator spectra for the input mode (dotted) and the two output modes (dashed) (b) the eigenenergy spectrum of the coupled system (figure 1) for the four modes coupled together inductively with the circuit parameters given in the text.

for the three em mode system then reads

$$H_t = H_s + \sum_{i=1}^3 (H_{e_i} - H_{e_{1s}}) \quad (3)$$

We can make a transformation using the unitary operator $T = \exp(i \sum x Q_s)$ to translate the SQUID Hamiltonian H_s into a more convenient form. The Hamiltonian

(2) can then be written as¹²

$$H_s^0 = T^\dagger H_s T = \frac{Q_s^2}{2C_s} + \frac{\phi_s^2}{2\phi_0} \sim \cos 2 \frac{\phi_s + \phi_0}{\phi_0} \quad (4)$$

where the ϕ_0 -periodic dependence of the (transformed) ring Hamiltonian on ϕ_s is explicit. This unitary transfor-

mation also modifies the ring-eld mode interactions to the form $H_{e_1s}^0 = \frac{e_1s}{s} s_{e_1}$ so that, following on from (3), the transformed system Hamiltonian (again ϕ -periodic in x) can be written as

$$H_t^0 = H_s^0 + \sum_{i=1}^3 H_{e_i} H_{e_1s}^0$$

Adopting this Hamiltonian we can solve the eigenproblem $H_t^0 |j_n\rangle = \epsilon_n |j_n\rangle$ and use the eigenvectors $|j_n\rangle$ to construct the evolution operator $U(t)$ for the system¹² via,

$$U(t) = \sum_n |j_n\rangle \exp\left(\frac{i\epsilon_n t}{\hbar}\right) \langle j_n| \quad (5)$$

The time averaged energy expectation values $\langle H_i \rangle$ for the ring and the eld modes can then be calculated from the expression

$$\langle H_i \rangle = \lim_{t \rightarrow \infty} \frac{1}{t} \int_0^t \text{Tr}[\rho_i(t) H_i] dt \quad (6)$$

where the $\rho_i(t)$ are the reduced density operators for the sub-components $i = e_1; e_2; e_3$ and s for the coupled system²⁹ which are obtained from the density operator $\rho(t) = U(t) \rho(0) U^\dagger(t)$ (for an initial density operator $\rho(0)$) by using $\rho_i(t) = \text{Tr}_{j \neq i} \rho(t)$.

A. Four mode (two photon) down conversion and entanglement

1. Without dissipation

Referring again to the system of figure 1, and assuming that it starts in an initial state $|j(0)\rangle$, the evolution operator (5) can then be used to generate the system state vector $|j(t)\rangle = U(t) |j(0)\rangle$ at any subsequent time t (from which $\rho(t)$ can be found via $\rho(t) = |j(t)\rangle \langle j(t)|$). As an illustration we now assume that the system, SQUID ring + oscillator modes, starts in the state $|j(0)\rangle = |j_{e_1}\rangle |j_{e_2}\rangle |j_{e_3}\rangle$; where $|j_{e_1}\rangle$ is the ground state of the ring and the $|j_{e_i}\rangle$ are the photon number states for the various eld modes of the system.

Starting in this initial state we show in figure 3(a) the time averaged energy expectation values of the eld modes (e_1 – the input and $e_{2,3}$ – the two outputs) of the system as a function of x , where the two outputs (e_2 and e_3) superimpose exactly, as is to be expected by symmetry. As is apparent, due to the interaction of the SQUID ring with e_1 , and one of the other two (output) modes e_2 and e_3 , sharp transition regions (or energy exchange regions¹²) develop in the time averaged energies, discussed by us in a previous publication¹². These regions of energy exchange between the ring and the eld modes occur over very narrow ranges in x , which is

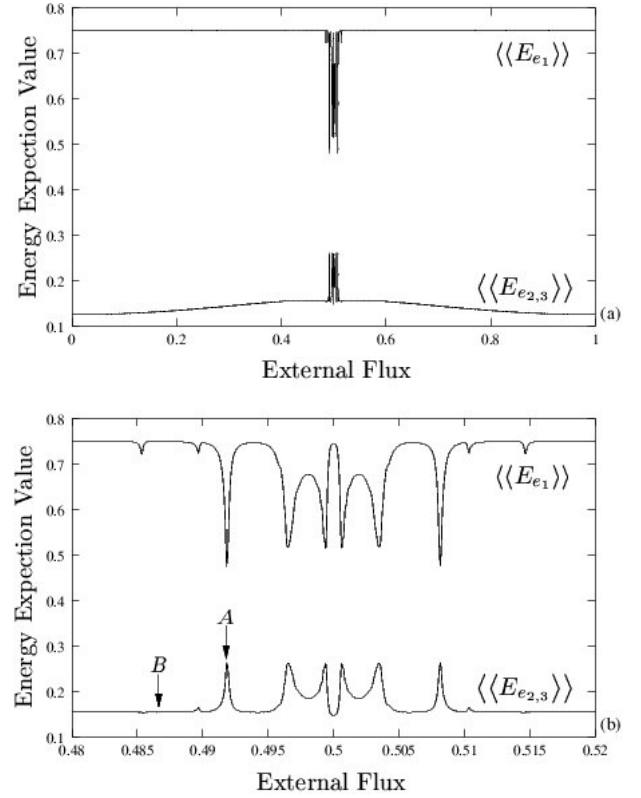


FIG. 3: (a) the time averaged energy expectation values for the electromagnetic input and output modes of the coupled system of figure 2 as a function of external bias flux (b) an zoomed in enlargement of the central section of the results in (a) as a function of bias flux showing a series of energy exchange regions; in the calculations presented subsequently the two bias points A and B have been selected, the former inside an exchange region, the latter outside.

clear from our example system in figure 3(a) and (b). As we shall demonstrate, the non-perturbative nature of the ring in these exchange regions is sufficient to generate photon down conversion and entanglement between the eld modes. In an earlier calculation¹² we showed that ring-eld mode interaction strength is a maximum at the centre of the exchange region and very small at its edge. For the calculations presented in this section we have chosen to bias the coupled system at the centre of the exchange region, denoted A in figure 3(b). The energy exchange region is seen as the energy splitting (divided crossing) circled in figure 2(b).

In figures 4(a) and (b) we show how the number expectation values $\langle n_{e_1} \rangle$, $\langle n_{e_2} \rangle$ and $\langle n_{e_3} \rangle$ of the three eld modes vary with the dimensionless time ($\tau = t/t_s$) for the bias points A and B in figure 3(b), where $x = 0.49183 \phi_0$ (at A in figure 4(a)) and $x = 0.487 \phi_0$ (at B in figure 4(b)). Here, we note first that for bias point A there is down conversion of energy from eld mode e_1 to one or other of the two half frequency ($\ell_{e_1}=2$) modes $e_{2,3}$ and second that $\langle n_{e_2} \rangle$ and $\langle n_{e_3} \rangle$ versus τ are iden-

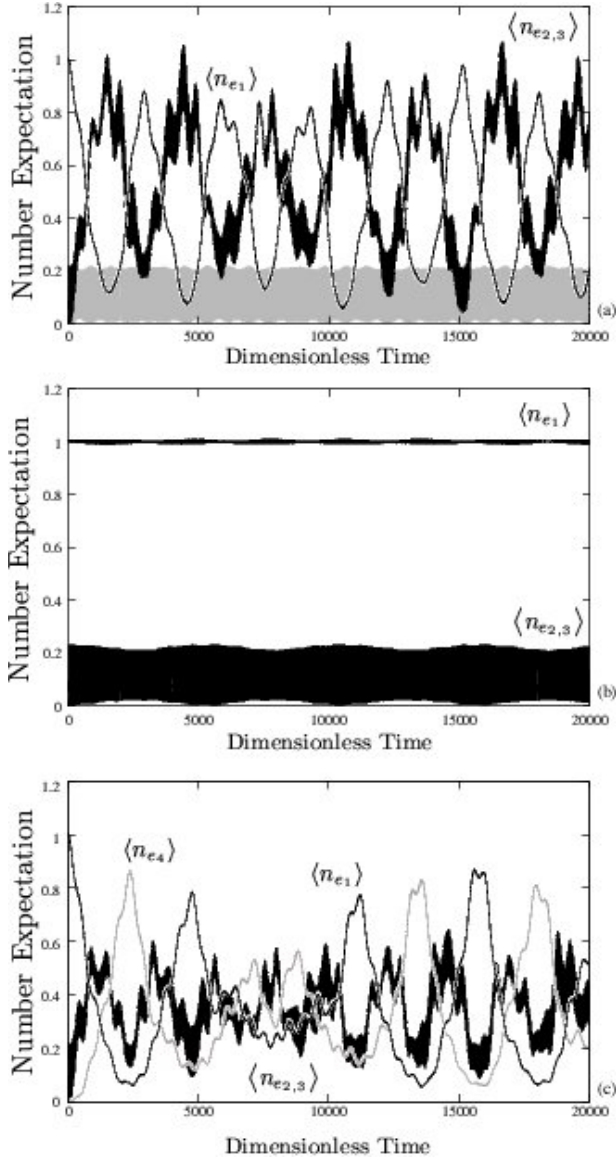


FIG. 4: (a) number expectation values for the electromagnetic input and output modes of the coupled system of figure 2 as a function of dimensionless time, at external flux point A in figure 3, starting with a photon occupancy of 1 in the input mode; also shown in grey is the output mode number expectation values for the zero photon occupancy in the input mode (b) the same results as (a) above calculated at the external bias flux point B in figure 3. (c) a repeat of the calculation of (a) with the inclusion of a third output mode e_4 , with its number occupancy shown in grey, at the same frequency as our input mode.

tical due to the symmetric nature of their coupling to the SQUID ring. In order to verify that the photon occupation of the $e_{2,3}$ modes is due to down conversion from mode e_1 , as stated above, we repeated our calculation at bias point A with the system in the initial state $j(0)_i = |j_{i_1}\rangle |j_{i_2}\rangle |j_{i_3}\rangle$. The time averaged

energies $\hbar\omega_{e_2}$ and $\hbar\omega_{e_3}$ for this situation are shown in grey in figure 4(a). As expected, with e_1 starting in state $|j_{i_1}\rangle$ there was no down conversion. However, we note that there is some occupancy in the output modes due to the ring-mode coupling energy available in the system. It is, of course, possible that higher harmonics of the output field oscillators could be excited, which may not be desirable. In order to investigate such excitations we have included an additional output mode, at the same frequency as the input mode, and recomputed the results of figure 4(a). This is shown in figure 4(c). Although it is apparent that the level of down conversion is reduced it is, however, still significant. It would appear, therefore, that the presence of unwanted higher harmonics in the output modes is a factor which might need to be reduced. Nevertheless, it does not negate the computations where such processes are not considered.

Concomitant with the two photon down conversion $e_1 \rightarrow e_{2,3}$ there exists the possibility that the photons in the lower frequency modes e_2 and e_3 are strongly correlated or even entangled. In order to characterise the correlations within this system we will employ two entropic quantities. The first of these yields information about the correlations that exist between any two components of a system^{12,30,31,32,33} and is defined by

$$I(A;B) = S_A + S_B - S_{AB} \quad (7)$$

where S_m is the von Neumann entropy for each subsystem (m)²⁴. We note that for a bipartite closed system this measure is often employed to characterise the entanglement present. However, complications arise when this quantity is used in multipartite or open systems (for more information see [34]). Nevertheless, it is still useful for gaining an appreciation of the correlations that are present between the components of the system in which we are interested. The second entropic quantity we shall use is the entanglement measure introduced by Adam and Cerf²², which for a subsystem A of the total system T is given by

$$E(A) = S_T - S_A \quad (8)$$

This measure has the important property that if it is negative definite then A is quantum correlated (i.e. entangled) with at least some of the rest of the system.

For this particular example we are interested in the correlations that exist between the two output mode, e_2 and e_3 . The computed entropy, $I(e_2;e_3) = S_{e_2} + S_{e_3} - S_{e_2,e_3}$, is shown in figure 5(a) as a function of dimensionless time for the bias points A and B in figure 3(b). In addition, in figure 5(b) we show the individual, and identical, entropies of the two (receiver) modes e_2 and e_3 with the initial field mode e_1 , i.e. $I(e_1;e_i) = S_{e_1} + S_{e_i} - S_{e_1,e_i}$, $i = 2$ or 3 for the same two bias points A and B. Figure 5(c) shows a repeat of the calculation of figure 5(a) having included an additional output mode at the same frequency as the input mode, as in figure 4(c). A gain, the inclusion of this extra output mode has modified the results. However, the two low frequency output modes (e_2

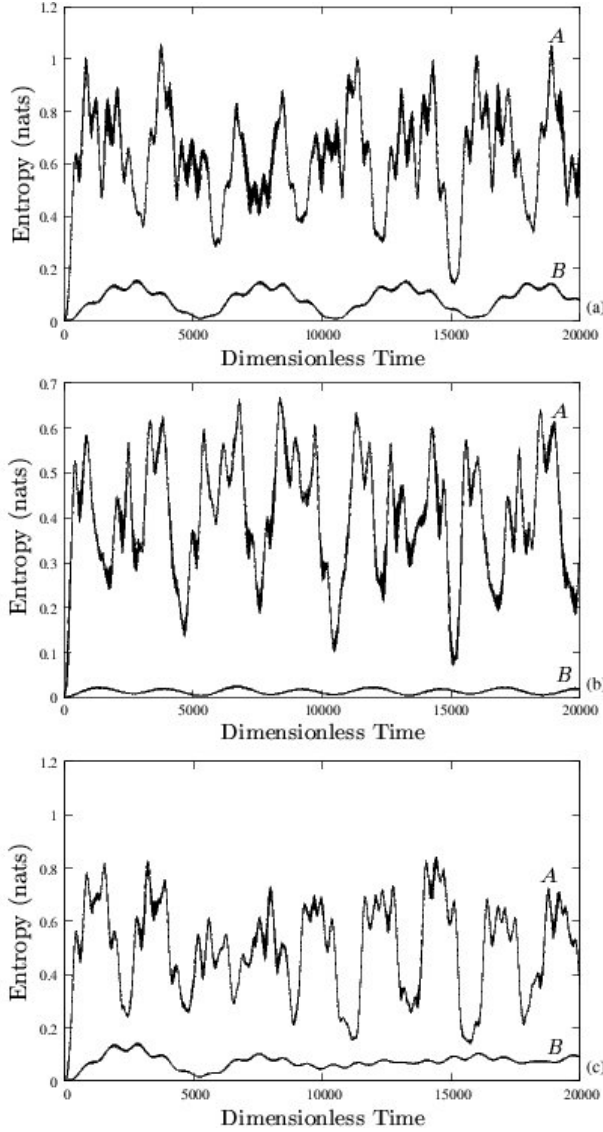


FIG. 5: (a) the entanglement entropy as function of dimensionless time between the two electromagnetic output modes of the system of figure 2 calculated at the bias flux points A and B in figure 3 (b). (b) the entanglement entropy between the input mode and one of the output modes as a function of dimensionless time, again calculated at the two bias points A and B in figure 3. (c) a repeat of the calculation of (a) modified by the inclusion of a third output mode at the same frequency as our input mode.

and e_3) are still significantly entangled with each other at the appropriate point in external flux, again indicating that the excitation of additional output modes reduces, but does not suppress, the entanglement in between the two low frequency output modes (e_2 and e_3). We note that the use of an actual LC^{15,16} circuit would altogether remove the need to consider higher order harmonics.

In the photon number expectation values of figure 4 it is apparent that the decrease in number expectation

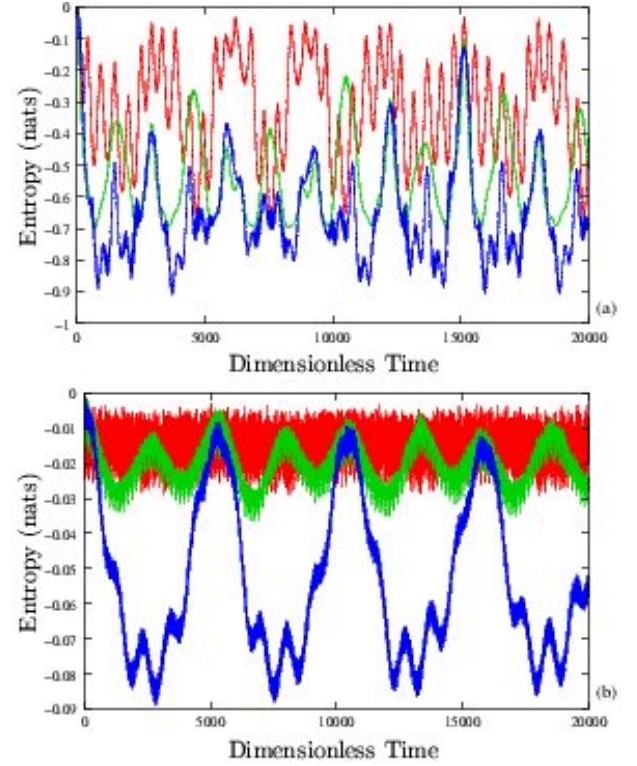


FIG. 6: (a) the A dam i-Cerf entanglement entropies for the coupled system of figure 2 as a function of dimensionless time calculated at point A in figure 3, where the SQUID ring results are in red, the input electromagnetic mode results are in green and those for the two output modes are in blue (b) the same calculation as above in (a) but now at the external bias flux point B in figure 3.

value of field mode e_1 is directly linked to its increase in modes e_2 and e_3 and that the degree of transfer is highly dependent on the value of ϕ_x in the exchange region. Correspondingly, from figure 5(a) it is clear that, with the SQUID ring biased into an exchange region, the correlations between the e_2 and e_3 modes are greatly affected by the choice of ϕ_x . Thus, at B the correlations are relatively close to zero at all times while at A it has a maximum of around 1.1. This ϕ_x -dependent variation in the strength of correlation is also seen in figure 5(b) between the e_1 and e_2 (or equivalently e_3) receiver mode. Again these correlations between each pair of coupled modes is identical, whether we choose bias point A or B. In order to characterise the quantum correlations with this system we show in figure 6 the A dam i-Cerf entanglement entropies for each mode of the system where, in figure 6(a), for bias point A in figure 3 (b), all four modes are entangled with the rest of the system throughout the evolution while in figure 6(b), while at bias point B, it is clear that the level of entanglement is much less. It is apparent in these figures that both the von Neumann and A dam i-Cerf approaches indicate that the level of entanglement of the modes in the total system can be con-

trolled by adjusting the external bias flux on the SQUID ring. The control over the entanglement which is manifest in figure 6 is to be compared to the case in quantum optics. Here, the optical media used are typically weakly (polynomially) non-linear as opposed to the extremely strong non-linear (non-perturbative) properties of the SQUID ring in an exchange region. Furthermore, these media generally couple weakly to em fields which does not have to be the case for SQUID rings. Most importantly, the strength of the ring-field interaction (with the resulting two photon down conversion and entanglement) in an exchange region can be varied by adjusting the bias flux on the ring. To the best of our knowledge, such control is very difficult to achieve with optical media.

$$\frac{d}{dt} = \frac{i}{\hbar} [H_t^0] + \sum_{sc} \frac{\gamma_{sc}}{2\hbar} (M_{sc} + 1) 2a_{sc} a_{sc}^\dagger - a_{sc}^\dagger a_{sc} - a_{sc} a_{sc}^\dagger \quad (9)$$

where M_{sc} is related to the temperature $T = 4.2K$, and frequency ω_{sc} , of each decohering bath for each subcomponent (sc) of the system via $M_{sc} = (\exp(\hbar\omega_{sc}/k_B T) - 1)^{-1}$. In equation (9) γ_{sc} is the coupling (i.e. the damping rate) between each of the system subcomponents and its respective bath. The choice to couple each subcomponent to a separate decohering bath is in keeping with the standard decoherence model used for open quantum systems³⁵. There is, of course, the possibility that in certain situations all the elements of this system could couple to a mutual decohering bath³⁶. This is an interesting scenario that would require a detailed analysis beyond the scope of this paper.

Following on from the entanglement entropy versus dimensionless time plots for the four mode system in the absence of dissipation (figure 6), we show in figures 7 and 8 the subcomponent (Landauer) entropies for two levels of dissipation, namely $\gamma = 10^{-5}\omega_s$ and $\gamma = 10^{-4}\omega_s$. As can be seen, in the less dissipative case shown in figure 7 (which would appear to be attainable experimentally^{9,37}) entanglement is maintained over a relatively long time period. However, as one would expect, over long enough times any original entanglement disappears. Nevertheless, for the case of figure 7 it appears that a useful level of entanglement is maintained amongst the output modes over a range of over 5000 in normalised time or 3×10^8 s in real time. This is considerably longer than the time constant corresponding to the $\omega_s C_s$ oscillator frequency of the SQUID ring, i.e. $1/2\pi \omega_s C_s^{-1} = 7 \times 10^{12}$ s for $\omega_s = 3 \times 10^{10}$ Hz and $C_s = 5 \times 10^{-15}$ F. Thus, provided the level of dissipation can be kept at or below this level it should prove possible to utilise this two photon entanglement in practical situations.

2. With dissipation

As has been discussed at great length in the literature³⁵ coupling of a quantum object to classical dissipative environments leads to decoherence over some characteristic time period. Clearly this is of great importance for any realistic discussion of entanglement in multipartite quantum systems. In order to model the effects of dissipation we have adopted the standard approach, very often used in the field of quantum optics. In this model the components of the system are coupled to decohering thermal baths. The master equation for the evolution of the density of the multi-component systems then has the form³⁵

$$a_{sc}^\dagger a_{sc} + \frac{\gamma_{sc}}{2\hbar} M_{sc} 2a_{sc}^\dagger a_{sc} - a_{sc}^\dagger a_{sc} - a_{sc} a_{sc}^\dagger \quad (9)$$

III. SIX MODE (FOUR PHOTON) DOWN CONVERSION

The scheme for a six mode system, consisting of one input oscillator mode (frequency $\omega_i = 2\omega_s$) and four identical output modes, all oscillating at one quarter of the input frequency, is shown diagrammatically in figure 9. Using the same procedure as we adopted in the case of the two photon down conversion described above, we have computed the number expectation values against normalised time for the input, the SQUID ring and the four output modes. These have been computed at the bias flux point A^0 in the centre of the exchange region (divided crossing) of figure 10. These expectation values are plot-

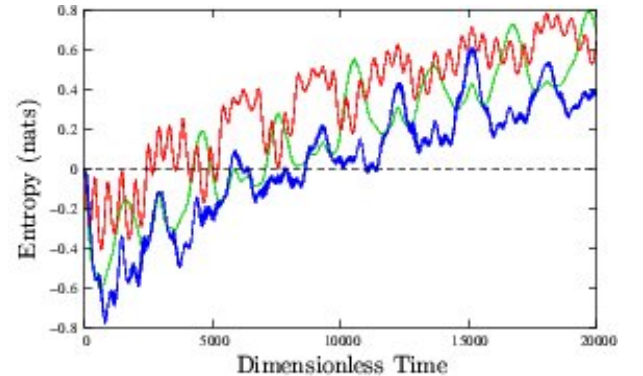


FIG. 7: Repeat of the calculation in figure 6(a) but now with dissipation introduced for $\gamma = 10^{-5}\omega_s$ with the colour coding green (input mode), blue (output mode) and red (SQUID ring).

ted in figure 11 for the input mode and the four output modes, each of which generates identical results. As can be seen, in the absence of dissipation the sum of the number expectation values for these output modes is reasonably close to 4, indicating that here the down conversion process via the SQUID ring is quite efficient. We note that the level of efficiency of this down conversion process decreases as the splitting frequency at the divided crossing increases. We suspect that this could be corrected if a sufficiently thorough review of the external flux dependence were to be undertaken. However, this is impractical to perform given the limitations on our current computational power.

The computational power required to generate accurate solutions for this four photon down conversion, and gain a detailed understanding of the correlations that exist between the components of the system, is extremely demanding. As with the two photon down conversion case, but even more so, the computational power at our disposal did not allow us to study the correlations between the four (identical) output modes of the system. What we have been able to do is to take any of the output photons, at a quarter of the frequency of the input photon, and show that each is strongly entangled with the rest of the system. By appealing to the earlier results presented in this paper, it is reasonable to assume that the four output modes are entangled with each other in addition to any entanglement with the input mode and the SQUID ring. The problem of describing, and quantifying, entanglement for systems of more than two quantum particles, is still a matter for serious debate^{38,39}. However, in a qualitative way, the computed results displayed in figure 12 suggest a practical route to the entanglement of many identical photon states through the intermediary of a highly non-perturbative SQUID ring medium. Again, with regard to the computational limits we faced, we were not able to introduce dissipation into the many moded system through a master equation of the type (9).

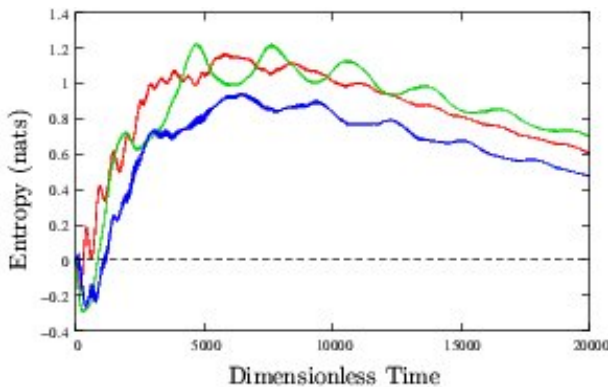


FIG. 8: Repeat of the calculation in figure 6(a) but now with dissipation introduced for $\alpha = 10^{-4} \text{ s}^{-1}$ with the colour coding green (input mode), blue (output mode) and red (SQUID ring).

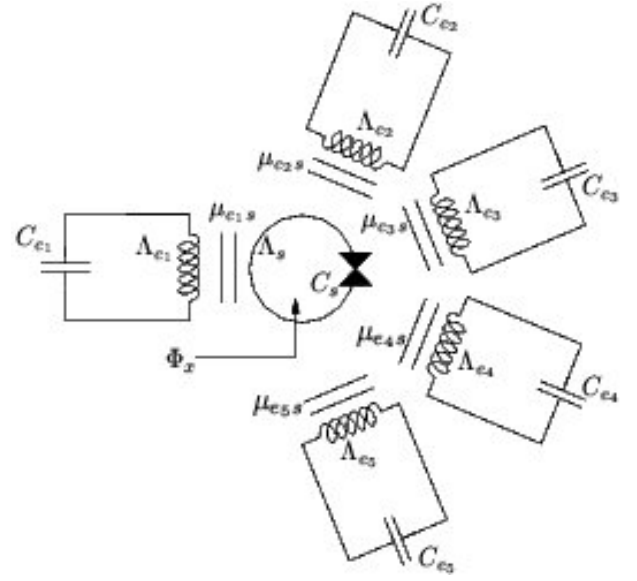


FIG. 9: Schematic for a six mode system with a mesoscopic quantum regime SQUID ring inductively coupled to one input and four output electromagnetic modes.

IV. HIGHER ORDER DOWN CONVERSION PROCESSES

Due to the limitations imposed by our computing power we have not been able to extend our investigations of entanglement beyond the six mode (four photon down conversion) range. Nevertheless, following the two and four photon processes we now consider a factor twenty down conversion process between an input and an output electromagnetic mode. For this calculation we have used the same SQUID ring parameters as before. However, with this calculation describing a factor twenty frequency conversion, the exchange regions have been redistributed as shown in figure 13. For the calculation presented in this section we have chosen to flux bias the ring at the centre of a particular exchange region in figure 13, denoted by A^0 . At this value of external flux we have been able to demonstrate quantum down conversion by a factor of twenty between the input and an output electromagnetic mode. In order to reduce the computational complexity of this calculation, and in contrast to the previous examples, we have taken $\alpha_{e1} = \alpha_s$ and assumed an initial (start) number occupancy in this input mode of βi_{e1} . In the computation we have inductively coupled the SQUID ring to an output oscillator mode at one twentieth of the input photon frequency. Setting the input and output coupling strengths at $\kappa = 0.01$, we should see, for a perfectly efficient down conversion process, that the number expectation value of the output modes reaches a peak of approximately 20 as a function of normalised time. The actual level of occupancy in the output mode is much lower than this potential maximum. However, as discussed earlier, the efficiency of this down conversion pro-

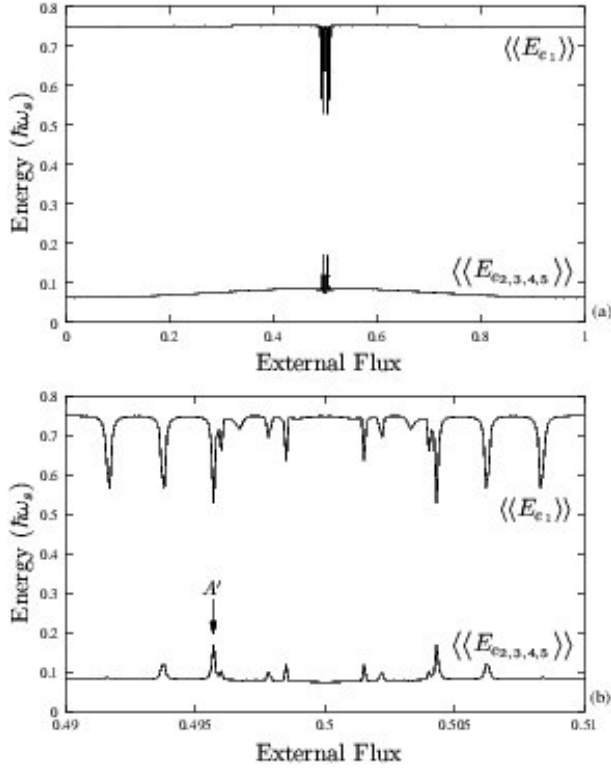


FIG. 10: (a) the time averaged energies at $T = 0K$ for the electromagnetic input and output modes of the coupled system of figure 9 as a function of external bias flux with the circuit parameters given in the text (b) a zoomed in enlargement of the central section of the results in (a) as a function of bias flux showing a series of energy exchange regions; in the calculations presented subsequently the bias point A^0 has been selected.

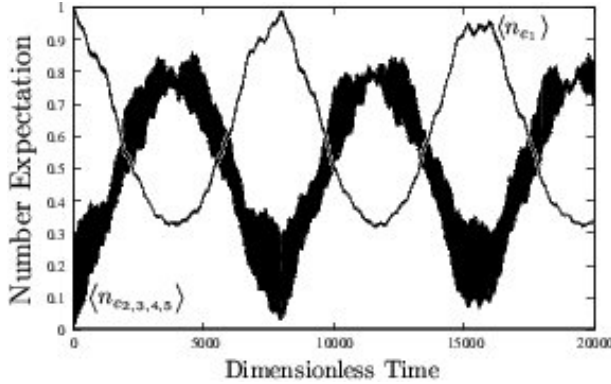


FIG. 11: Number expectation values for the electromagnetic input and output modes of the coupled system of figure 9 as a function of dimensionless time, at external flux point A^0 in figure 10, starting with a photon occupancy of 1 in the input mode.

cess is greatly affected by the value of the external bias flux chosen. The results presented in figure 14 are, for the

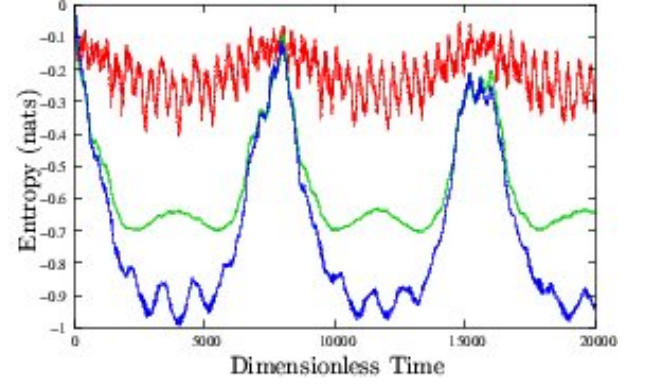


FIG. 12: The Adam-Cerf entanglement entropies of the coupled system of figure 9 as a function of dimensionless time calculated at point A^0 in figure 10, where the SQUID ring results are in red, the input electromagnetic mode results are in green and those for the two output modes are in blue.

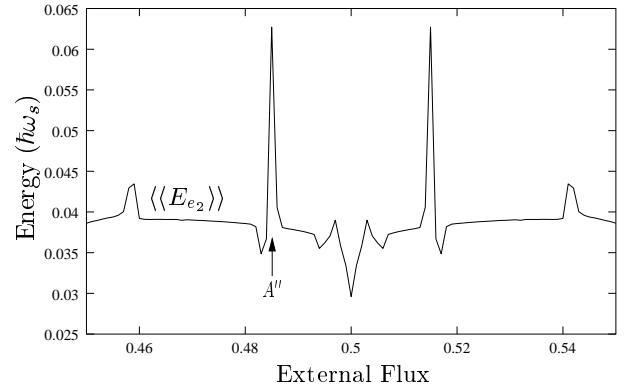


FIG. 13: The $T = 0K$ time averaged energy for the output electromagnetic mode of a factor 20 SQUID ring mediated down conversion process as a function of external bias flux where the bias point A^0 in an energy exchange region is used in subsequent calculations with the circuit parameters given in the text.

moment, the best that could be obtained within the practical time and computational constraints imposed on us. In figure 14 the number expectation value for the output oscillator mode (e_2) is plotted as a function of normalised time. This confirms that, at least from a theoretical viewpoint, high order down conversion (and, by implication, up conversion) processes can occur between input and output modes through the intermediary of a quantum regime SQUID ring. It should be noted that while the occupancy of the lower frequency output mode here is not very efficient, it is still a non-trivial deviation from zero. It is therefore still valid to look upon this result as evidence that SQUID rings in the quantum regime can mediate high order down conversion, even if, for the moment, at low rates of efficiency. By extension, if the computational power were available to us, it seems reasonable

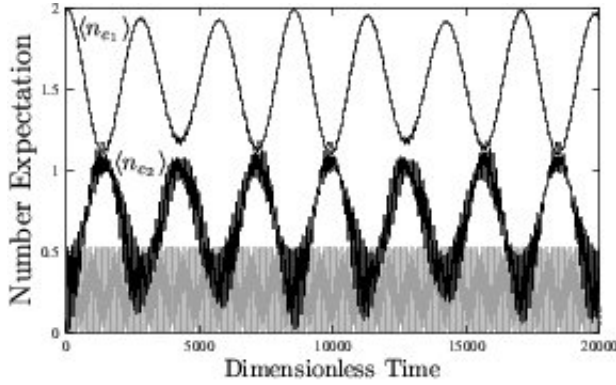


FIG. 14: Number expectation values for the electromagnetic input and output modes of the coupled system of figure 13 as a function of dimensionless time, at external flux point A⁰⁰ in this figure, starting with a photon occupancy of 2 in the input mode; also shown in grey is the output mode number expectation values for the zero photon occupancy in the input mode.

to assume that (i) we could obtain the same result if we were to couple twenty output modes to the SQUID ring and (ii) that there is every possibility that these output modes would be able to entangle with each other. Furthermore, given the extremely non-perturbative nature of a quantum mechanical SQUID ring, we might expect that, with the appropriate experimental arrangements in place, down conversion frequency ratios much higher than 20 might be observed.

V. CONCLUSIONS

The exhibitability afforded by this ϕ_x -dependent control (tunability) of the maximum coupling strength, and the temporal form of the entanglements within ring-eld mode(s) system, raises interesting possibilities. This control might be of great advantage in the preparation of qubits in quantum computing and quantum information processing^{1,2}. Our calculations point to a method for generating a wide range of levels of entanglement between photon states (or, in general, any quantum circuits coupled to the SQUID ring) with only very small adjustments in bias flux required. This we consider to be the important outcome of this work. To give an example, for bias point A in the data of figures 5(a) and (b) the time evolution shows instances, such as at $t = 10;000$, when the entanglement entropy $I(e_2; e_3)$ is high and the entanglement entropy $I(e_1; e_4)$, $i = 2$ or 3, is low. Even more significantly, in figure 7 we see

that at dimensionless times such as $t = 5000$ the output modes are the only modes which are unequivocally entangled. This would appear to be of significance in many proposed device applications^{1,2,28,40} where a way is needed to use a known input to prepare a set of entangled photons and then to disconnect the input, without significantly disrupting the entanglement so produced. We note that in many experimental situations^{30,31,32,33} any readjustment of output entanglement requires the development of a new system setup. Many of the ideas explored in this work were inspired by concepts in quantum optics. In fact, there are strong similarities between a quantum regime SQUID ring and a device frequently employed in quantum optics – the non-linear optical coupler – this being formed from two or more linearly coupled waveguides where at least one is composed of an optically non-linear medium^{41,42,43,44,45}. However, there are two important differences between optical couplers and the SQUID ring: (i) optical non-linear interactions usually have a non-resonant character and (ii) optical non-linear couplers are difficult to make because of the strict phase and frequency matching conditions that must be obeyed by all involved processes simultaneously. Hence, it may well be that SQUID ring coupled devices, such as those presented here, could lead to a feasible way of realising (or at least simulating) non-linear optical couplers.

The manipulation of the different entanglements in the model systems considered in this paper, based on just one SQUID ring, appears to open up the possibility of creating more sophisticated, multi-SQUID ring based, circuit networks where the constituent elements could be entangled and disentangled as required simply by changing bias fluxes. Obviously further work is called for to determine how newly entanglement properties can be manipulated in more complex systems. As a pointer to the use of such complex systems, we have already shown in this work that flux controlled, two photon down conversion ($1_1 \rightarrow 2_{2,3}$ where $1_1 = 2_{2,3}$) and entanglement can occur in a SQUID ring mediated system as can four photon down conversion ($e_1 \rightarrow e_{2,3,4,5}$). Given the cosine nonlinearity of the ring, we would expect the entanglement of even more photon states to be possible although to demonstrate this is beyond the limits of the current computational power available to us.

VI. ACKNOWLEDGEMENTS

We would like to express our thanks to the Engineering and Physical Sciences Research Council for the support of this work through its Quantum Circuits Network Initiative.

Electronic address: t.d.clark@sussex.ac.uk

¹ H.K.Lo, S.Popescu, and T.P.Spiller, eds., Introduction

to Quantum Computation and Information (World Scientific, New Jersey, 1998).

- ² D. Bouwmeester, A. Ekert, and A. Zeilinger, *The Physics of Quantum Information* (Springer, 2000).
- ³ P. Shor, *Proc. 35th Annual Symposium on the Foundations of Computer Science*, p. 124 (IEEE Computer Society, Los Alamitos, Ca., 1994).
- ⁴ L. K. Grover, *Proc. 28th Annual ACM Symposium on Theory of Computing*, p. 212 (ACM Press, York, 1996).
- ⁵ C. H. van der Wal, A. C. J. ter Haar, F. K. Wilhelm, R. N. Schouten, C. J. P. M. Hamans, T. P. Orlando, S. Lloyd, and J. E. Mooij, *Science* 290, 773 (2000).
- ⁶ J. R. Friedman, V. Patel, W. Chen, S. K. Tolpygo, and J. E. Lukens, *Nature* 406, 43 (2000).
- ⁷ Y. Nakamura, C. D. Chen, and J. S. Tsai, *Phys. Rev. Lett.* 79, 2328 (1997).
- ⁸ Y. Nakamura, Y. A. Pashkin, and J. S. Tsai, *Nature* 398, 786 (1999).
- ⁹ A. Lupascu, C. J. M. Verwijs, R. N. Schouten, C. J. P. M. Hamans, and J. E. Mooij, *Phys. Rev. Lett.* 93, 177006 (2004).
- ¹⁰ T. P. Spiller, *Fortschritte Phys.-Prog. Phys.* 48, 1075 (2000).
- ¹¹ I. Chiorescu, P. Bertet, K. Semba, Y. Nakamura, C. J. P. M. Hamans, and J. E. Mooij, *Nature* 431, 159 (2004).
- ¹² M. J. Everitt, T. D. Clark, P. Stiehl, H. P. Rance, R. J. P. Rance, A. Vourdas, and J. F. Ralph, *Phys. Rev. B* 64, 184517 (2001).
- ¹³ M. O. Scully and M. S. Zubairy, *Quantum Optics* (Cambridge, 1997).
- ¹⁴ M. J. Everitt, P. Stiehl, T. D. Clark, A. Vourdas, J. F. Ralph, H. P. Rance, and R. J. P. Rance, *Phys. Rev. B* 63, 144530 (2001).
- ¹⁵ R. Whiteman, T. D. Clark, R. J. P. Rance, H. P. Rance, V. Schollman, J. F. Ralph, E. M. J., and J. Diggins, *J. Mod. Opt.* 45, 1175 (1998).
- ¹⁶ A. Walra, D. I. Schuster, A. Blais, L. Frunzio, R. S. Huang, J. Majer, S. Kumar, S. M. Girvin, and R. J. Schoelkopf, *Nature* 431, 162 (2004).
- ¹⁷ J. B. Majer, F. G. Paauw, A. C. J. ter Haar, C. J. P. M. Hamans, and J. E. Mooij, *Phys. Rev. Lett.* 94, 090501 (2005).
- ¹⁸ A. J. Berkley, H. Xu, R. C. Ramos, M. A. Gubrud, F. W. Strauch, P. R. Johnson, J. R. Anderson, A. J. Dragt, C. J. Lobb, and F. C. Wellstood, *Science* 300, 1548 (2003).
- ¹⁹ M. D. Kim and J. Hong, *Phys. Rev. B* 70, 184525 (2004).
- ²⁰ H. Xu, F. W. Strauch, S. K. Dutta, P. R. Johnson, R. C. Ramos, A. J. Berkley, H. Paik, J. R. Anderson, A. J. Dragt, C. J. Lobb, et al., *Phys. Rev. Lett.* 94, 027003 (2005).
- ²¹ M. R. Geller and A. N. Cleland, *Phys. Rev. A* 71, 032311 (2005).
- ²² N. J. Cerf and C. Adam, *Phys. Rev. Lett.* 79, 5194 (1997).
- ²³ A. J. G. Hey, ed., *Feynman and Computation* (Westview Press, Boulder, Colorado, 1999).
- ²⁴ M. A. Nielsen and I. L. Chuang, *Quantum Computation and Quantum Information* (Cambridge University Press, 2000).
- ²⁵ M. J. Everitt, T. D. Clark, P. Stiehl, H. P. Rance, R. J. P. Rance, and J. F. Ralph, *quant-ph/0307181* (2003).
- ²⁶ T. P. Spiller, T. D. Clark, R. J. P. Rance, and A. W. Idom, *Prog. Low Temp. Phys.* 13, 219 (1992).
- ²⁷ Y. Srivastava and A. W. Idom, *Phys. Rep.-Rev. Sec. Phys. Lett.* 148, 1 (1987).
- ²⁸ T. P. Orlando, J. E. Mooij, L. Tian, C. H. van der Wal, L. S. Levitov, S. Lloyd, and J. J. M. Azo, *Phys. Rev. B* 60, 15398 (1999).
- ²⁹ C. Cohen-Tannoudji, B. Diu, and F. Laloe, *Quantum Mechanics Vol. I*, p. 298 (Wiley, New York, 1986).
- ³⁰ G. Lindblad, *Commun. Math. Phys.* 33, 305 (1973).
- ³¹ E. H. Leib, *Bull. Am. Math. Soc.* 81, 1 (1970).
- ³² A. W. Ehrl, *Rev. Mod. Phys.* 50, 221 (1978).
- ³³ S. M. Barnett and S. J. D. Phoenix, *Phys. Rev. A* 44, 535 (1991).
- ³⁴ A. J. Scott, *Phys. Rev. A* 69, 052330 (2004).
- ³⁵ U. Weiss, *Quantum Dissipative Systems* (World Scientific, Singapore, 1999).
- ³⁶ T. Yu and J. H. Eberly, *Phys. Rev. B* 66, 193306 (2002).
- ³⁷ J. M. Martinis, S. Nam, J. Aumentado, and C. Urbina, *Phys. Rev. Lett.* 89, 117901 (2002).
- ³⁸ V. M. Kendon, K. Nemoto, and W. J. Munro, *J. Mod. Opt.* 49, 1709 (2002).
- ³⁹ P. Rungta, W. J. Munro, K. Nemoto, P. D. Eu, G. J. Milburn, and C. M. Caves, *arXiv:quant-ph/0001075 v2* (2000).
- ⁴⁰ Y. Makhlin, G. Schon, and A. Shnirman, *Nature* 398, 305 (1999).
- ⁴¹ D. M. Ogilevtsev, N. Korolkova, and J. Perina, *J. Mod. Opt.* 44, 1293 (1997).
- ⁴² J. Rahacek, L. Mista, J. Fiurasek, and J. Perina, *Phys. Rev. A* 65, 043815 (2002).
- ⁴³ J. Fiurasek and J. Perina, *Phys. Rev. A* 62, 033808 (2000).
- ⁴⁴ J. A. Armstrong, N. B. Lembergen, J. D. Cuing, and P. S. Pershan, *Phys. Rev.* 127, 1918 (1962).
- ⁴⁵ C. Silberhom, P. K. Lam, O. Weib, F. Konig, N. Korolkova, and G. Leuchs, *Phys. Rev. Lett.* 86, 4267 (2001).